How does non-covalent Se···Se=O interaction stabilize selenoxides at naphthalene 1,8-positions: structural and theoretical investigations†

Satoko Hayashi,[a] Waro Nakanishi,*[a] Atsushi Furuta,[a] Jozef Drabowicz,[b] Takahiro Sasamori[c] and Norihiro Tokitoh[c]

Received (in Montpellier, France) 9th June 2008, Accepted 25th September 2008
First published as an Advance Article on the web 17th November 2008
DOI: 10.1039/b809763a

Bis-selenides (LL), such as 8-[MeSe(X)]-1-[MeSe(Z)]$C_{10}H_6$ (**1**(LL)), 8-[EtSe(X)]-1-[EtSe(Z)]$C_{10}H_6$ (**2**(LL)), 8-[*p*-YC_6H_4Se(X)]-1-[MeSe(Z)]$C_{10}H_6$ (**3**(LL)) and 8-[*p*-YC_6H_4Se(X)]-1-[*p*-YC_6H_4Se(Z)]$C_{10}H_6$ (**4**(LL)) were oxidized with ozone at 0 °C, where (X, Z) = (lone pair, lone pair) for LL. Bis-selenoxides, **1**(OO), **3**(OO) and **4**(OO) where (X, Z) = (oxygen, oxygen), were obtained in the oxidation of **1**(LL), **3**(LL) and **4**(LL), respectively, *via* corresponding selenide-selenoxides, **1**(LO), **3**(LO) and **4**(LO), respectively. A facile Se–C bond cleavage was observed in **2**(LL). The structures of **1**(LO) and **1**(OO) were determined by the X-ray analysis. Three Se···Se=O atoms in **1**(LO) and four O=Se···Se=O atoms in **1**(OO) align linearly. While the non-covalent Se···Se=O 3c–4e interaction operates to stabilize **1**(LO), the non-covalent O=Se···Se=O 4c–4e interaction would not stabilize **1**(OO). The 3c–4e interaction must play an important role to control the stereochemistry of selenoxides. The 8-G-1-[$MeSe(OH)_2$]$C_{10}H_6$ (***n***(OH·OH)) are the key intermediates in the racemization of 8-G-1-[MeSe(O)]$C_{10}H_6$ (***n***(O)) in solutions, where G = SeMe (**1**), H (**5**), F (**6**), Cl (**7**) and Br (**8**). Energies of ***n***(OH·OH), relative to ***n***(O), are evaluated based on the theoretical calculations. G of SeMe is demonstrated to operate most effectively to protect from racemization of selenoxides among ***n*** = **1** and **5–8**, since the relative energies for G of *cis*- and *trans*-SeMe are largest.

Introduction

Selonoxides[1–4] [RSe(O)R′] afford optically active enantiomers, as well as sulfoxides,[5,6] if R and R′ are not the same, since Se in each selenoxide is three-coordinated containing a lone pair. However, it is usually difficult to utilize optical active selenoxides to introduce the optical activity in a target molecule,[1,2,4,7] since the racemization of optical active selenoxides is usually very fast. Nevertheless, some efforts have been made to stabilize the stereochemistry of selenoxides, by taking advantage of non-covalent coordination by the neighboring groups (G) of the G···Se=O type.[2,4,7]

Naphthalene 1,8-positions supply a good system to investigate such interactions, since the non-bonded distances between heteroatoms at the positions are close to the sum of the van der Waals radii minus 1 Å.[8,9] Various types of non-covalent interactions are detected in naphthalene 1,8-positions.[8–11] The σ-type three center-four electron interactions (σ(3c–4e)),[12–14] σ(2c–4e),[12] π(2c–4e),[12] distorted π(2c–4e),[12] and Z_4 4c–6e[13] are typical examples. Such non-covalent interactions are demonstrated to control the fine structures of molecules.[15] Recently, we investigated fine structures of 8-G-1-(arylseleninyl)-naphthalene with G = H, F, Cl and Br, together with the factors to control the structures, as the first step to control the stereochemistry of selenoxides.[16] The factors are called G, O and Y dependences, which originate from the n_p(G)···σ*(Se–O), n_p(O)···π(Nap) and n_p(O)···π(Ar) interactions, respectively.[16]

We paid much attention to G = MeSe and ArSe in 8-G-1-(arylseleninyl)naphthalenes, since many conformers are plausible around the two Se–C_{Nap} bonds, relative to the case of G = H and halogens. Scheme 1 shows the orbitals taking part in the non-covalent Se···Se=O interaction. A bis-selenide

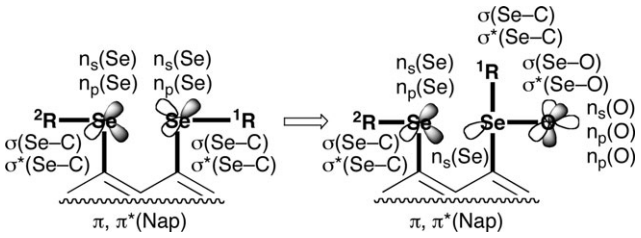

Scheme 1 Orbitals taking part in the non-bonded Se···Se=O interactions in naphthalene 1,8-positions.

[a] *Department of Material Science and Chemistry, Faculty of Systems Engineering, Wakayama University, 930 Sakaedani, Wakayama 640-8510, Japan. E-mail: nakanisi@sys.wakayama-u.ac.jp; Fax: +81 73 457 8253; Tel: +81 73 457 8253*
[b] *Center of Molecular and Macromolecular Studies, Polish Academy of Science, Sienkiewicza, 112, 90-363 Lodz, Poland*
[c] *Institute for Chemical Research, Kyoto University, Gokasho, Uji, Kyoto 611-0011, Japan*

† Electronic supplementary information (ESI) available: Energies and relative energies for 8-G-1-[MeSe(X)]$C_{10}H_6$ [G = MeSe (**1**), H (**5**), F (**6**), Cl (**7**) and Br (**8**) with X = lone pair (L), O (O), OH^+ (OH^+) and O_2H_2(OH·OH)], the packing structures of **1**(OO), counter map for **1**(OO), Cartesian coordinates for optimized structures of **1** and **5–8** with X = lone pair (L), O (O), OH^+ (OH^+) and O_2H_2(OH·OH)]. CCDC reference numbers 688690 (**1**(LO)) and 688691 (**1**(OO)). For ESI and crystallographic data in CIF or other electronic format see DOI: 10.1039/b809763a

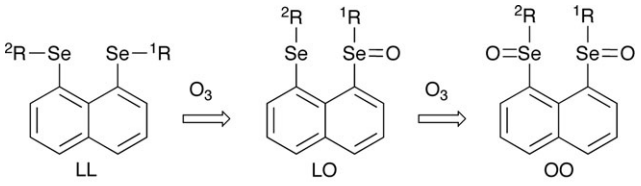

1 (^{1}R = ^{2}R = Me), **2** (^{1}R = ^{2}R = Et), **3** (^{1}R = Me, ^{2}R = Ar), **4** (^{1}R = ^{2}R = Ar)
Ar = Ph (**a**), *p*-MeOC$_6$H$_4$ (**b**), *p*-*t*BuC$_6$H$_4$ (**c**) and *p*-O$_2$NC$_6$H$_4$ (**d**)

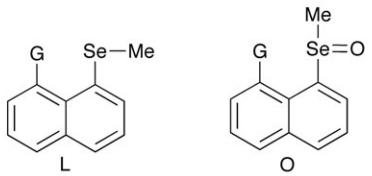

5 (G = H), **6** (G = F), **7** (G = Cl) and **8** (G = Br)
(L = lone pair and O = oxide)

Chart 1 Bis(selanyl)naphthalenes, **1–4**, together with **5–8**.

contains double n_s(Se), n_p(Se), σ(Se–C) and σ*(Se–C) orbitals. However, n_s(O), n_p(O), $n_{p'}$(O), σ(Se–O) and σ*(Se–O) appear newly with the quit of an n_p(Se), when a selenide-selenoxide is formed from the bis-selenide.

The oxidation and formation of 8-[^{2}RSe(X)]-1-[^{1}RSe(Z)]C$_{10}$H$_6$ (**1** (^{1}R = ^{2}R = Me), **2** (^{1}R = ^{2}R = Et), **3** (^{1}R = Me, ^{2}R = *p*-YC$_6$H$_4$: Y = H (**a**), MeO (**b**) and NO$_2$ (**d**)) and **4** (^{1}R = ^{2}R = *p*-YC$_6$H$_4$: Y = H (**a**) and *t*Bu (**c**)) are investigated for LL where (X, Z) = (lone pair, lone pair), LO (lone pair, oxygen) and OO (oxygen, oxygen) (Chart 1). The reactions are easily controlled and each process is followed by the spectroscopic method. Non-bonded O=Se···Se=O interactions are also the subject of interest.

The structures around the naphthyl group (Nap) in 8-G-1-RSeC$_{10}$H$_6$ are well explained by three types, type **A** (**A**), **B** and **C**.[8c,d,f–h,17,18] The combined notation are used to specify the structures of **1–4** with G = RSe, where the notation, such as **AA**, **BA** or **CA**, shows the conformers around the two C_{Nap}–Se bonds. Scheme 2 draws the notations employed in this work, exemplified by **1**(LO).

The structures of **1**(LO) and **1**(OO) are determined by X-ray crystallographic analysis. Quantum chemical (QC) calculations are performed on **1**(LO) and **1**(OO), to elucidate the role of the Se···Se=O interaction in **1**(LO) and the O=Se···Se=O interaction in **1**(OO) as the factor to control the fine structures. Orbitals of two Se atoms in **1**(LO) and **1**(OO) must overlap directly with each other, which would stabilize the fine structures. QC calculations are also

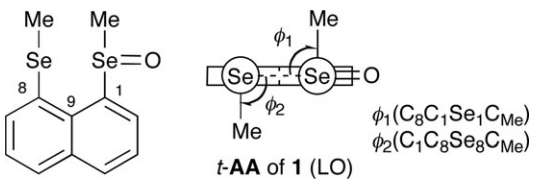

A: 60° < ϕ_1, ϕ_2 < 105°; **A'**: 255° < ϕ_1, ϕ_2 < 300°
B: 150° < ϕ_1, ϕ_2 ≤ 180°; **B'**: 180° < ϕ_1, ϕ_2 < 210°
C: 105° ≤ ϕ_1, ϕ_2 ≤ 150°; **C'**: 210° ≤ ϕ_1, ϕ_2 ≤ 255°

Scheme 2 Structures around naphthyl group in 8-G-1-[RSe(X)]C$_{10}$H$_6$, exemplified by **1**(LO).

performed on 8-G-1-[MeSe(X)]C$_{10}$H$_6$ [G = MeSe (**1**), H (**5**), F (**6**), Cl (**7**) and Br (**8**) with X = lone pair (L), O (O), OH$^+$ (OH$^+$) and O$_2$H$_2$ (OH·OH)], where OH·OH must be the key intermediate in the racemization of **1** and **5–8**, in the presence of a trace of water. The relative energy [ΔE = E(***n***(OH·OH)) − (E(***n***(O)) + E(H$_2$O)) (***n*** = **1** and **5–8**)] is evaluated: that for G = MeSe is largest among them. The larger value must correspond to a selenoxide with the stronger resistance for racemization, although ***n***(OH·OH) is not the transition state. The G···Se=O interactions containing the Se···Se=O and O=Se···Se=O interactions are also analyzed with the natural orbital (NBO)[19,20] and atoms-in-molecules (AIM)[21,22] analyses.

Oxidation of 1,8-bis(selanyl)naphthalenes (LL) with ozone is well controlled and monitored, which gives 1,8-bis(seleninyl)-naphthalenes (OO) *via* 8-selanyl-1-seleninylnaphthalenes (LO). Factors to control the fine structures of **1**(LO) and **1**(OO) are clarified based on QC calculations, after determination of the structures. The Se···Se=O interaction is demonstrated to control the fine structure of **1**(LO), whereas the role of the O=Se···Se=O interaction in **1**(OO) is critically discussed. The role of G in **1** and **5–8** in the racemization process is also evaluated.

Results and discussion

Survey of oxidation

Bis-selenides (***n***(LL): ***n*** = **1–4**) were oxidized with ozone in the methylene dichloride solution of each bis-selenide at 0 °C. The bis-selenides (***n***(LL)) gave corresponding bis-selenoxides (***n***(O)) *via* corresponding selenide-selenoxides (***n***(LO)), except for **2**(LL). While **1**(LL) gave **1**(LO), followed by the quantitative formation of **1**(OO), a facile Se–C bond cleavage occurred on the oxidation of **2**(LL), resulting in the formation of naphtho-1,8-[*c,d*]-1,2-diselenole (**9**).[23] β-Elimination of the selenoxide may be responsible for the facile Se–C bond cleavage. In the case of **3**(LL), the methylselanyl Se atoms were attacked exclusively. **3**(LO) were consumed to produce the corresponding **3**(OO) with more ozone. **4**(LO) were also produced from the corresponding **4**(LL) with ozone, followed by the formation of the corresponding **4**(OO), respectively. The results are summarized in Chart 1. The reactions are well followed by NMR.

Structures of 1(LO) and 1(OO)

Single crystals of **1**(LO) and **1**(OO) were obtained *via* slow evaporation of methylene dichloride-hexane solutions and one of suitable crystals was subjected to X-ray crystallographic analysis for each compound.[24] Only one type of structure corresponds to each of **1**(LO) and **1**(OO) in the crystals. Table 1 shows the crystallographic data of **1**(LO) and **1**(OO). Fig. 1 shows the structures of **1**(LO) and **1**(OO).[25] The packing structure of **1**(OO) is shown in Fig. S1 of the Electronic Supplementary Information (ESI†). Selected interatomic distances, angles and torsional angles of the compounds **1**(LO) and **1**(OO) are collected in Table 2, together with those of **1**(LL), which contains two types, **1**(LL)$_A$ and **1**(LL)$_B$.[26]

Table 1 Crystallographic data for **1**(LO) and **1**(OO)

	1(LO)	**1**(OO)
Empirical formula	$C_{12}H_{12}OSe_2$	$C_{12}H_{12}O_2Se_2{\cdot}2.5H_2O$
Formula weight	330.14	391.18
Temperature/K	298(2)	103(2)
Crystal system	Monoclinic	Monoclinic
Space group	$P2_1/n$ (#14)	$C2/c$ (#15)
a/Å	5.8460(19)	25.549(9)
b/Å	14.473(3)	5.8653(18)
c/Å	14.1490(16)	20.850(8)
β/°	97.660(17)	117.329(4)
V/Å^3	1186.5(5)	2775.6(16)
Z	4	8
D_c/g cm^{-3}	1.848	1.872
F(000)	640	1544
Reflections observed [$I > 2\sigma(I)$]	2200	2435
Parameters	136	190
R_1 [$I > 2\sigma(I)$]	0.032	0.021
R_1 [all data]	0.082	0.022
ωR_2 [$I > 2\sigma(I)$]	0.065	0.053
ωR_2 [all data]	0.077	0.054
Goodness-of-fit on F^2	1.029	1.109

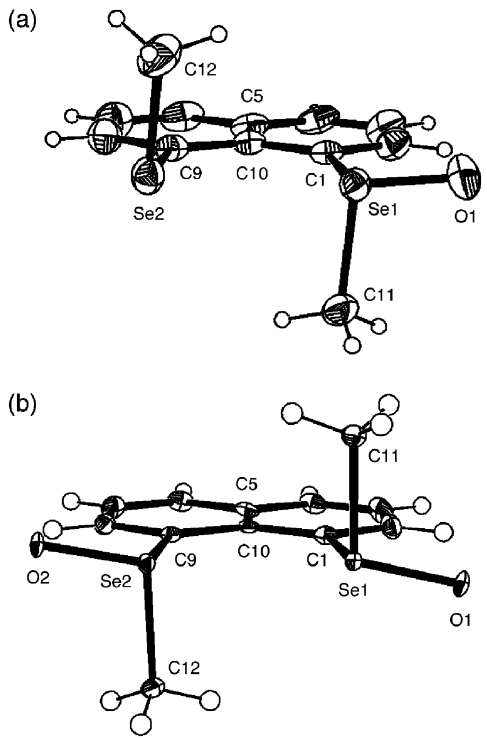

Fig. 1 Structures of **1**(LO) (a) and **1**(OO) (b) with atomic numbering scheme for selected atoms (thermal ellipsoids are shown at the 50% probability level).

The structures of **1**(LO) and **1**(OO) are all **AA** for two methyl groups (Fig. 1 and Table 2).[15] The planarity of the naphthyl (Nap) planes is very good. All Se–O bonds are placed in the naphthyl plane. The superior tendency of the Se–O bonds to stay on the naphthyl plane (O dependence)[16] must be the driving force for the structures of **1**(LO) and **1**(OO). Three Se···Se–O atoms align linearly ($\angle$SeSeO = 173.31(15)°) and the Se–O bond is almost perpendicular to another $C_{Nap}SeC_{Me}$ plane in **1**(LO). The non-covalent n_p(Se)···σ*(Se–O) 3c–4e interaction operates effectively to keep the Se–O bond on the naphthyl plane in **1**(LO) (G dependence).[16] These results show that the structure of **1**(LO) is well stabilized by the O and G dependences observed in 1-naphthyl selenoxides.[16]

On the other hand, there is no n_p(Se) in **1**(OO). Therefore, the G dependence of the n_p(Se)···σ*(Se–O) type cannot operate in **1**(OO). Consequently, the driving force for the structure must come from the O dependence for both Se–O bonds. Namely, the non-covalent O–Se···Se–O σ(4c–4e) interaction must be carefully examined as a factor to stabilize the fine structure of **1**(OO), although the non-bonded Se···Se distances are less than the sum of van der Waals radii by *ca.* 0.65 Å.[27] The σ(4c–4e) interaction seems not so important.

How does G of MeSe control the fine structure and the behavior? QC calculations are performed on **1** and **5–8**.

QC calculations

QC calculations were performed on **1**(LO) with the B3LYP/6-311+G(d) method of the Gaussian 98 program.[28–30] QC calculations revealed energy profiles of the compounds.[31] Table 3 collects the results of the QC calculations. The NBO analysis[19,20] were performed on **1**(LO) and **1**(OO) with the B3LYP/6-311+G(d) method. The results are shown in Table 4. The AIM parameters[21,22] are calculated for **1**(LO) and **1**(OO) with the Gaussian 03 program[32] employing the 6-311+G(3df) basis sets for Se with the 6-311+G(3d,2p) basis sets for C and H at the B3LYP level. They are analyzed employing the AIM 2000 program.[33] Table 5 collects the results of AIM calculations.

Indeed, the results of QC calculations essentially correspond to those in the gas phase, but the factors to control and/or stabilize the structures in gas phase must also operate in solid states and in solutions. Therefore, it must be instructive to consider those predicted by QC calculations, although we must be careful for the crystal packing effect in crystals and the solvent effect in solutions, since such effects often larger than the predicted factors.

The effect of G to stabilize 8-G-1-[MeSe(X)]$C_{10}H_6$ [G = MeSe (**1**), H (**5**), F (**6**), Cl (**7**) and Br (**8**) with X = lone pair (L), O (O), OH^+ (OH^+) and O_2H_2 (OH·OH)] will be discussed in detail, here. The results clarified the factors for the racemization of selenoxides. ***n***(OH·OH) (***n*** = **1** and **5–8**) must be the key intermediates in the racemization of ***n***(O), in the presence of (a trace of) water in solutions.

Effect of G in 1 and 5–8

Racemization of an optically active selenoxide is believed to proceed *via* a selenide dihydroxide (***n***(OH·OH)).[4a–d] Scheme 3 shows a hypothetical racemization process of optically active ***n***(O*) *via* ***n***(OH·OH).

Protonation of ***n***(O*) occurs at O of an optically active isomer of ***n***(O*: R) to give ***n***(O*H^+: R) at the initial stage of the reaction. ***n***(OH·OH) will form in the reaction of ***n***(O*H^+: R) with water followed by the deprotonation to yield ***n***(OH·OH). Elimination of water from ***n***(OH·OH) results in the racemization, since of ***n***(OH·OH) is not optically active as a whole. Similar reactions occur starting from ***n***(O*: S) to yield ***n***(OH·OH) *via* ***n***(O*H^+: S), which also leads to racemization.

Table 2 Selected interatomic distances (Å), angles (°) and torsional angles (°) around Se atom in **1** (LO) and **1** (OO), together with those of **1** (LL)

	1 $(LL)_A$[a]	**1** $(LL)_B$[a]	**1** (LO)	**1** (OO)
Interatomic distances				
Se1–Se2	3.051(4)	3.064(4)	3.1587(10)	3.1512(8)
Se1–C1	1.929(4)	1.932(3)	1.983(5)	1.959(2)
Se1–C11	1.944(4)	1.953(4)	1.954(5)	1.940(2)
Se1–O1			1.653(4)	1.6771(15)
Se2–C9	1.926(4)	1.932(4)	1.928(5)	1.970(2)
Se2–C12	1.944(4)	1.949(4)	1.938(6)	1.934(2)
Se2–O2				1.680(15)
Angles				
Se2–Se1–C11	164.47(3)	146.46(3)	85.93(16)	88.26(7)
Se2–Se1–O1			173.31(15)	167.54(5)
Se1–Se2–C12	150.34(3)	159.73(3)	85.65(18)	89.41(7)
Se1–Se2–O2				167.51(5)
Se1–C1–C10	122.9(3)	123.9(3)	126.9(4)	124.33(16)
C1–Se1–C11	99.29(16)	98.41(16)	96.0(2)	94.73(9)
C1–Se1–O1			101.1(2)	102.69(8)
C11–Se1–O1			100.7(2)	102.85(9)
Se2–C9–C10	123.9(3)	122.9(3)	124.1(4)	124.67(16)
C9–Se2–C12	99.27(16)	98.50(16)	98.1(2)	93.38(9)
C9–Se2–O2				102.21(8)
C12–Se2–O2				102.29(9)
C1–C10–C9	126.4(3)	127.2(3)	127.0(4)	128.1(2)
Torsional angles				
Se1–C1–C10–C5	173.5(2)	−176.0(2)	−177.6(4)	179.19(15)
C10–C1–Se1C11	−154.1(3)	136.8(3)	82.8(4)	−86.49(19)
C10–C1–Se1–O1			−175.0(4)	169.19(17)
Se2–C9–C10–C5	172.2(2)	−170.2(2)	178.8(4)	178.90(15)
C10–C9–Se2–C12	−138.8(3)	148.0(3)	84.6(4)	−87.10(19)
C10–C9–Se2–O2				169.54(18)
O1–Se1–Se2–O2				140.3(3)

[a] Ref. 26.

Table 3 Energies and relative energies for 8-G-1-[MeSe(O_iH_j)]$C_{10}H_6$ (i, j = 0, 1 and 2)[a]

Form	O: **A**/**AA**[b]	OH^+: **A**/**AA**[b]	OH·OH: **AC**
5 (G = H)	−2902.0303	−2902.4017	−2978.4686
Qn(Se)	1.309	1.307	1.324
Qn(O)	−0.968	−0.837	−0.996, −0.993
Qn(H)		0.497	0.433, 0.433
+W[c]	−2978.4741	−2978.2198	−2978.4686
Δ[d,e]	as 0.0	667.7 (as 0.0)	14.4 (as 0.0)
6 (G = F)	−3001.3000	−3001.6744	−3077.7371
+W[c]	−3077.7438	−3077.4925	−3077.7371
Δ[d,e]	as 0.0	659.8 (−7.9)	17.6 (3.2)
7 (G = Cl)	−3361.6478	−3362.0250	−3438.0833
+W[c]	−3438.0916	−3437.8431	−3438.0833
Δ[d,e]	as 0.0	652.4 (−15.2)	21.8 (7.4)
8 (G = Br)	−5475.5651	−5475.9442	−5552.0007
+W[c]	−5552.0089	−5551.7623	−5552.0007
Δ[d,e]	as 0.0	647.4 (−20.2)	21.5 (7.1)
1 (G = *trans*-MeSe)	−5342.8896	−5343.2854	−5419.3241
+W[c]	−5419.3334	−5419.1035	−5419.3241
Δ[d,e]	as 0.0	603.6 (−64.1)	24.4 (10.0)
1 (G = *cis*-MeSe)	−5342.8869	−5343.2821	−5419.3214
+W[c]	−5419.3307	−5419.1002	−5419.3214
Δ[d,e]	as 0.0[f]	612.3 (−55.4)	31.5 (17.1)

[a] Calculated with the B3LYP/6-311+G(d) method. [b] **A** for **5–8** and **AA** for **1**. [c] Evaluated based on the values of $E(H_2O_2)$ = −151.5891 au, $E(H_2O)$ = −76.4438 au and $E(OH^-)$ = −75.8181 au calculated with the same method. [d] Relative to that of the corresponding ***n***(O): **A**. [e] Relative to the same structure derived from **5** (G = H) being given in parenthesis. [f] 7.1 kJ mol^{-1} from the corresponding species of **1** (G = *trans*-MeSe; O): **AA**.

Table 4 Second order perturbation energies in the donor (D)–acceptor (A) interactions of the n(G)···σ*(Se–O) type in 8-G-1-[MeSe(O)]-$C_{10}H_6$ and 8-G-1-[$MeSe^+$(OH)]$C_{10}H_6$, calculated with the NBO method[ab]

D; A	n_p(G); σ*(Se–O)	n_p(G): σ*(Se^+–OH)
G = F	1.44	9.15 (0.87)[c]
G = Cl	3.29	13.65 (1.09)[c]
G = Br	3.73	27.95 (1.19)[c]
G = *cis*-SeMe	4.77[d]	34.99 (1.76)[c]
G = *trans*-SeMe	5.52	41.86 (2.69)[c]
G = *trans*-SeMe[e]	5.86	
G = *trans*-Se(O)Me[e]	1.53 (×2)[f]	

[a] The 6-311+G(d) basis sets being employed. [b] In kcal mol^{-1}. [c] Corresponding to the n_s(G)···σ*(Se^+–OH) interaction. [d] 0.76 kcal mol^{-1} for the n_s(Se)···σ*(Se–O) type interaction. [e] The 6-311+G(3df) basis sets being employed for Se with the 6-311+G(3d,2p) basis sets for C and H. [f] Corresponding to the n_s(Se)···σ*(Se–O) interactions.

Table 5 Second order perturbation energies in the donor–acceptor interactions of the n(G)···σ*(Se–O) type at the naphthalene 1,8-positions in **1** (LO) and **1** (OO), calculated with the NBO method[a]

Compound	r_o(Se, Se)/Å	$\rho_b(\boldsymbol{r}_c)/ea_o^{-3}$	$\Delta\rho_b(\boldsymbol{r}_c)/ea_o^{-5}$	$H_b(\boldsymbol{r}_c)$/au
1 (LO)	3.2521	0.0195	0.0420	−0.0005
1 (OO)	3.2851	0.0160	0.0393	0.0002

[a] The 6-311+G(3df) basis sets being employed for Se and the 6-311+G(3d,2p) basis sets for C and H.

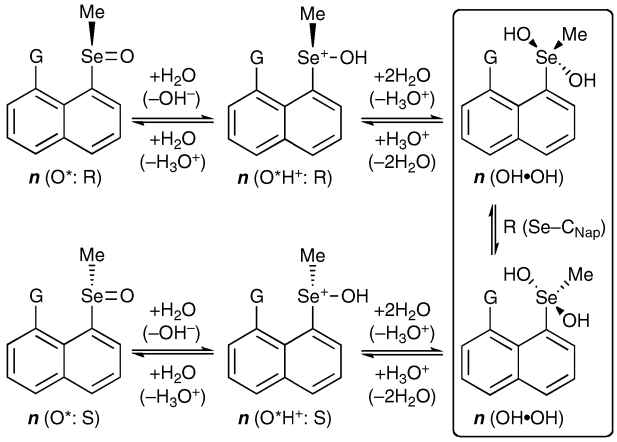

Scheme 3 Mechanism for racemization of ***n***(O*) *via* ***n***(OH·OH) (***n*** = **1** and **5–8**).

Water may originate from the solvent and the racemization would proceed under the neutral conditions. The stability of ***n***(OH·OH) must affect on the rates of racemization for the optical active selenoxides.

The effect of G on the stability of 8-G-1-[MeSe(O_iH_j)]$C_{10}H_6$ [**1** and **5–8**: L ($i = j = 0$), O ($i = 1, j = 0$), OH^+ ($i = j = 1$) and OH·OH ($i = j = 2$)] are examined based on the QC calculations. The results of QC calculations performed with the B3LYP/6-311+G(d) method are collected in Table 3. Table 3 also contains natural charges (*Qn*) of Se and O calculated employing the natural population analysis.[20] Scheme 4 shows optimized structures of the global minimum for each of **1**(LL), **1**(LO) and **1** (LOH^+), together with the three types, **AA′**, **BB** and **AC**, for **1** (LOH·OH). The values for **AC** of ***n***(LOH·OH) are given in Table 3, since **AC** is most stable among the three for each.[34]

Energy differences of the reactions in Scheme 3 are examined based on the values shown in Table 3. The energy of ***n***(O) + H_2O (E(***n***(O) + H_2O)) is taken as the standard for each, for convenience of comparison. How are the selenoxides stabilized by G at the 8-position? The effect of G on the stabilization of selenoxides is examined before discussion the energy profile shown in Scheme 3.

Eqn (1) shows the energies of ***n***(L) + H_2O_2 (E(***n***(L) + H_2O_2)) relative to E(***n***(O) + H_2O) [ΔE(***n***(LO) = E(***n***(L) + H_2O_2) − E(***n***(O) + H_2O)) (see Table S1 in the ESI†). Similarly, eqn (2) and (3) exhibit ΔE(***n***(OH^+)) and ΔE(***n***(OH·OH)),[35] respectively, which are defined as [E(***n***(OH^+) + HO^-) − E(***n***(O) + H_2O)] and [E(***n***(OH·OH)) − E(***n***(O) + H_2O)], respectively.[36]

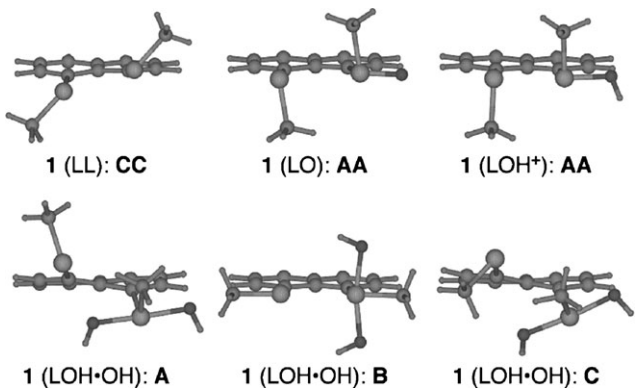

Scheme 4 Optimized structures for **1** (G = SeMe) and the derivatives.

$$\Delta E(\boldsymbol{n}(\mathrm{LO})) = E(\boldsymbol{n}(\mathrm{L}) + H_2O_2) - E(\boldsymbol{n}(\mathrm{O}) + H_2O)$$
$$G = H\ (121.8\ \mathrm{kJ\ mol^{-1}}) < F\ (131.3) < \textit{cis}\text{-MeSe}\ (133.9) < Cl\ (136.8) \leq Br\ (137.6) < \textit{trans}\text{-MeSe}\ (141.0) \quad (1)$$

$$\Delta E(\boldsymbol{n}(OH^+)) = E(\boldsymbol{n}(OH^+) + HO^-) - E(\boldsymbol{n}(\mathrm{O}) + H_2O)$$
$$G = H\ (667.7\ \mathrm{kJ\ mol^{-1}}) > F\ (659.8) > Cl\ (652.4) > Br\ (647.4) \gg \textit{cis}\text{-MeSe}\ (605.2) > \textit{trans}\text{-MeSe}\ (603.6) \quad (2)$$

$$\Delta E(\boldsymbol{n}(\mathrm{OH{\cdot}OH})) = E(\boldsymbol{n}(\mathrm{OH{\cdot}OH})) - E(\boldsymbol{n}(\mathrm{O}) + H_2O)$$
$$G = H\ (14.4\ \mathrm{kJ\ mol^{-1}}) < F\ (17.6) < Cl\ (21.8) \approx Br\ (21.5) < \textit{trans}\text{-MeSe}\ (24.4) < \textit{cis}\text{-MeSe}\ (31.5) \quad (3)$$

The order in eqn (1) corresponds the energy lowering effect by the G···Se–O interactions in the formation selenoxides relative to the G···Se–C interactions in selenides. However, we must be careful to examine the values for G = *cis*-MeSe and *trans*-MeSe, since the structure of the corresponding selenide is commonly **CC** (see Table S1 in the ESI†).

Eqn (2) exhibits that the protonation on the seleninyl O atom occurs more easily in the order of G = H < F < Cl < Br ≪ *cis*-MeSe < *trans*-MeSe. The results show that the protonation occurs more easily when G become better donors, especially for G = MeSe. The evaluated ΔE(***n***(OH^+)) values are very large in magnitudes, however, they do not mean that the process is very difficult to occur. The large magnitudes are the results of the calculations for the charge separated species of the ***n***(OH^+) + HO^- type. Only the relative values are important, since protonation will occur easily in solutions. Resulting hypervalent n_p(G)···σ*(Se–OH^+) interactions stabilize further the species in the order shown in eqn (2), relative to the case of the selenoxides.

The activation energies for the racemization of optically active selenoxides are closely related to the values shown in eqn (3), although they are the energies for the intermediates, ***n***(OH·OH). The activation energies are expected to increase in this order. The activation energy for G = *cis*-MeSe is predicted to be larger than that with *trans*-MeSe. However, *cis*-MeSe and *trans*-MeSe isomers interconvert with each other. Therefore, it may be better to evaluate the value by G = *trans*-MeSe under the experimental conditions: The activation energy of **1**(LO) with G = MeSe is estimated to be about 10 kJ mol^{-1} larger than that of **5** (L) with G = H and the former is also larger than the case of G = Br by *ca.* 3 kJ mol^{-1}. Fig. 2 summarizes the effect of G given in eqn (2).

G at the 8-position will protect sterically from the racemization of an optical active ***n***(O*). G must stabilize the optical active ***n***(O*) and the protonated ***n***(O*H^+) whereas G would destabilize ***n***(OH·OH). The steric congestion at the backside of the Se^+–OH bond in ***n***(O*H^+) by G will block the space for H_2O to attack to produce ***n***(OH·OH) (Scheme 4). We must be careful, since G could also stabilize ***n***(OH·OH) in some

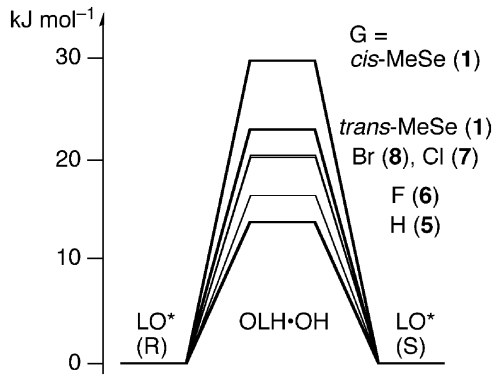

Fig. 2 Energies of $\boldsymbol{n}$(OH·OH), relative to $\boldsymbol{n}$(O) for $\boldsymbol{n}$ = **1** and **5–8**.

cases. The calculated values might correspond to the total effects of the electronic and steric effects. Energy profiles for the racemization evaluated by above calculations must contain main factors. The energies for the transition states must be close to those of the intermediates, $\boldsymbol{n}$(OH·OH).

NBO analysis for n(G)···σ*(Se–O) interactions

Table 4 summarizes the second order perturbation energies ($E(2)$) for the charge transfer (CT) interactions of the n(G)···σ*(Se–O) type in 8-G-1-[MeSe(O)]$C_{10}H_6$ and 8-G-1-[$MeSe^+$(OH)]$C_{10}H_6$ evaluated with the NBO method.[37] The B3LYP/6-311 + G(d) method is employed for the calculations. The $E(2)$ values becomes larger in an order shown in eqn (4).

$$E(2)\text{: G = F (1.44) < Cl (3.29) < Br (3.73) < } cis\text{-MeSe (4.77) < } trans\text{-MeSe (5.52)} \quad (4)$$

The $E(2)$ values are also evaluated for **1**(LO) and **1**(OO), employing the 6-311 + G(3df) basis sets for Se and the 6-311 + G(3d,2p) basis sets for C and H at the B3LYP level.[38] Table 4 also contains the values. The n_p(G)···σ*(Se–O) interaction are evaluated to be 5.9 kcal mol^{-1} for **1**(LO)[39] and as 1.5 (× 2) kcal mol^{-1} for the n_s(G)···σ*(Se–O) interactions in **1**(OO). The larger value for **1**(LO) relative to **1**(OO) implies the more effective interaction of the n_p(G)···σ*(Se–O) type in **1**(LO). The contribution of the 4c–4e interaction of the O–Se···Se–O type was not detected by the NBO analysis. Fig. 3 summarizes the interactions.

The nature of the n_p(G)···σ*(Se–O) interaction in **1**(LO) and the n_s(G)···σ*(Se–O) interactions in **1**(OO) are evaluated based on the AIM analysis, next.

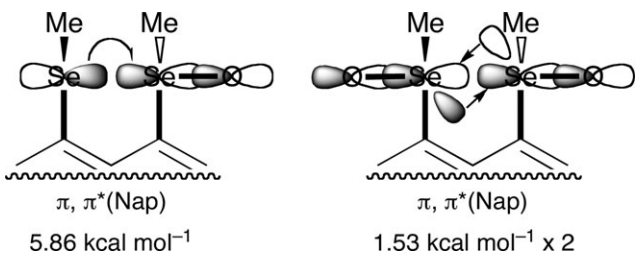

Fig. 3 The n_p(G)···σ*(Se–O) interaction in **1**(LO) and the n_s(G)···σ*(Se–O) interactions in **1**(OO) evaluated by the NBO method.

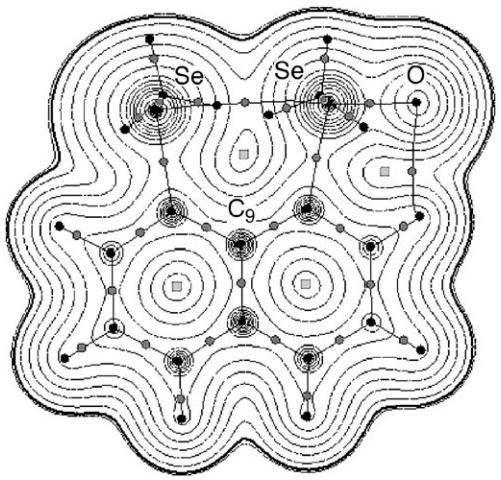

Fig. 4 Contour map of $\rho_b(\boldsymbol{r}_c)$ for **1**(LO) in the $SeSeC_9$ plane, together with BCPs (●), ring critical points (■) and bond paths. The contours [ea_o^{-3}] are at 2^l (l = ±8, ±7,...0) and 0.0047 (heavy line). Two Me groups are located upside and downside of the $SeSeC_9$ plane. The C_2, C_3, C_6 and C_7 atoms with the C–H bonds deviate substantially from the plane.

AIM analysis of 1(LO) and 1(OO)

The AIM analysis are carried out on **1**(LO) and **1**(OO). The 6-311 + G(3df) basis sets are employed for Se and the 6-311 + G(3d,2p) basis sets for C and H at the B3LYP level. Table 5 collects the AIM parameters of **1**(LO) and **1**(OO) for the bond critical points (BCPs: $\boldsymbol{r}_c$) on the interaction lines between non-bonded Se atoms.

The low values of electron densities at BCPs ($\rho_b(\boldsymbol{r}_c)$) in **1**(LO) and **1**(OO) (0.016–0.020 ea_o^{-3}) show that the interactions are ionic in nature. Laplacian values of $\rho_b(\boldsymbol{r}_c)$ ($\Delta\rho_b(\boldsymbol{r}_c)$) are both positive, whereas the total electron energy densities at BCPs ($H_b(\boldsymbol{r}_c)$) for **1**(LO) is negative but it is positive for **1**(OO). The results strongly suggest that the n_p(G)···σ*(Se–O) interaction in **1**(LO) is the CT interaction in nature similarly to the case of $R_2Se\cdots Br_2$ (MC) but the n_s(G)···σ*(Se–O) interactions in **1**(OO) seems weaker than such CT interactions.[40]

Fig. 4 shows the counter map of $\rho_b(\boldsymbol{r}_c)$ in the $SeSeC_9$ plane for **1**(LO), together with BCPs (●), ring critical points (■), bond paths and the interaction lines. BCP are detected on the Se···Se and O···^{2}H interaction lines. The BCP on the Se···Se interaction line well visualize the n_p(Se)···σ*(Se–O) interaction in **1**(LO). While BCP is also detected on the O···^{2}H interaction line, the interaction is very small. A similar counter map is also drawn for **1**(OO), which is shown in Fig. S2 of the ESI.†

Conclusion

X-Ray crystallographic analysis of 8-methylselanyl-1-(methylseleninyl)naphthalene (**1**(LO)) and 1,8-bis(methylseleninyl)-naphthalene **1**(OO) revealed that the three Se···Se=O atoms in **1**(LO) and the four O=Se···Se=O atoms in **1**(OO) align linearly. All Se–O bonds are placed in the naphthyl plane. The superior tendency for the Se–O bonds to stay on the naphthyl plane (O dependence) must be the

driving force for the fine structures of **1** (LO) and **1** (OO). The noncovalent $n_p(Se)\cdots\sigma(Se–O)$ 3c–4e interactions (G dependence) operate effectively to stabilize the structure of **1** (LO). On the other hand, the driving force for the structure of **1** (OO) must mainly come from the O dependence for each Se–O bond in **1** (OO), since the G dependence cannot operate without $n_p(Se)$.

QC calculations clarify the factors that protect from racemization of selenoxides. The energies of 8-G-1-[$MeSe(OH)_2$]-$C_{10}H_6$ from (8-G-1-[MeSe(O)]$C_{10}H_6$ + H_2O) are shown to be in an order of G = H (14.4 kJ mol^{-1}) < F (17.6) < Cl (21.8) ≈ Br (21.5) < *trans*-SeMe (24.4) < *cis*-SeMe (31.5). The activation energies for the racemization should increase in this order, since 8-G-1-[$MeSe(OH)_2$]$C_{10}H_6$ must be the key intermediates. The activation energy of **1** (LO: G = MeSe) is evaluated to be larger than that of **5** (L: G = H) and **8** (L: G = Br) by 10 and 3 kJ mol^{-1}, respectively. The results will help to design the optically stable selenoxides. The NBO and AIM analyses support the discussion and visualize the interactions.

Investigations on the chiral **3a** (LO), prepared in the oxidation of **3a** (LL) with chiral reagents, are in progress. Details will be reported elsewhere.

Experimental

General considerations

Manipulations were performed under an argon atmosphere with standard vacuum-line techniques. Glassware was dried at 130 °C overnight. Solvents and reagents were purified by standard procedures if necessary. Melting points were determined on a Yanaco MP-S3 melting point apparatus and uncorrected. NMR spectra were recorded at room temperature on a JEOL AL-300 spectrometer (^1H, 300 MHz; ^{13}C, 75 MHz) and on a JEOL Lambda-400 spectrometer (^1H, 400 MHz; ^{77}Se, 76 MHz). The ^1H, ^{13}C and ^{77}Se NMR spectra were recorded in $CDCl_3$. Chemical shifts are given in ppm relative to Me_4Si for the ^1H and ^{13}C NMR spectra and relative to reference compound MeSeMe for the ^{77}Se NMR spectra. Column chromatography was performed by using silica gel (Fujishilysia PSQ-100B) and basic alumina (E. Merck) and analytical thin layer chromatography was performed on precoated silica gel plates (60F-254) with the systems (v/v) indicated.

Syntheses

Bis(methylselanyl 1,8-bis(methylselanyl)naphthalene (1 (LL)). To a solution of the dianion of naphtho[1,8-*c,d*]-1,2-diselenole, which was prepared by reduction of the diselenole **9**[23] (1.03 g, 3.64 mmol) with $NaBH_4$ in an aqueous THF solution, was added methyl iodide (1.29 g, 9.06 mmol) at room temperature. After a usual workup, the crude was purified by column chromatography (flash column, SiO_2, hexane). Recrystallization of the chromatographed product from hexane gave **1** (LL) as colorless prisms in 98% yield, mp 85.0–85.5 °C, ^1H NMR (300 MHz, $CDCl_3$, δ, ppm, TMS): 2.33 (s, 6H), 7.32 (t, 2H, J = 7.7 Hz), 7.70 (dd, 2H, J = 1.2 and 8.2 Hz), 7.73 (dd, 2H, J = 1.2 and 7.5 Hz); ^{13}C NMR (75 MHz, $CDCl_3$, δ, ppm, TMS): 13.3, 125.7, 128.3, 131.9, 132.3, 135.3, 135.6; ^{77}Se NMR (76 MHz, $CDCl_3$, δ, ppm, Me_2Se): 231.4. Anal. Calc. for **1** (LL) ($C_{12}H_{12}Se_2$): C, 45.88; H, 3.85%. Found: C, 45.73; H, 3.77%.

8-Methylselanyl-1-(methylseleninyl)naphthalene (1 (LO)). **1** (LL) (0.98 mg, 3.12 mmol) was dissolved in 20 mL of CH_2Cl_2 and the solution was bubbling with the ozone for 5 min. TLC was checked for the completion of the reaction (rf = 0.07 (chloroform)). Then the solution was evaporated and dried *in vacuo*. The crude product was purified by column chromatography (flash column, Al_2O_3, CH_2Cl_2). **1** (LO) gave 85% yield as colorless powder, mp 129.8–130.1 °C; ^1H NMR (400 MHz, $CDCl_3$, δ, ppm, TMS): 2.29 (s, 3H), 2.78 (s, 3H), 7.48 (t, J 7.6 Hz, 2H), 7.76 (t, J 7.7 Hz, 2H), 7.98–8.05 (m, 2H), 8.10 (dd, J 1.1 and 7.2 Hz, 1H), 8.88 (dd, J 1.2 and 7.4 Hz, 1H); ^{13}C NMR (75 MHz, $CDCl_3$, δ, ppm, TMS): 13.87, 41.12, 125.73, 126.28, 126.35, 126.57, 131.01, 132.44, 133.06, 136.13, 138.93, 141.34; ^{77}Se NMR (76 MHz, $CDCl_3$, δ, ppm, Me_2Se): 210.8, 833.0. Anal. Calc. for **1** (LO) ($C_{12}H_{12}OSe_2$): C, 43.66; H, 3.66%. Found: C, 43.61; H, 3.60%.

1,8-Bis(methylseleninyl)naphthalene (1 (OO)). **1** (LL) (0.58 g, 0.30 mmol) was dissolved in 20 mL of CH_2Cl_2 and the solution was bubbling with the ozone for 15 min. TLC was checked for the completion of the reaction (rf = 0.00 (chloroform)). Then the solution was evaporated and dried *in vacuo*. The crude product was purified by column chromatography (flash column, Al_2O_3, CH_2Cl_2). **1** (OO) gave 59% yield as colorless powder, mp 154.8–155.2 °C; ^1H NMR (400 MHz, $CDCl_3$, δ, ppm, TMS): 2.71 (s, 6H), 7.84 (t, J 7.7 Hz, 2H), 8.18 (dd, J 1.2 and 6.9 Hz, 2H), 8.71 (dd, J 1.4 and 6.9 Hz, 2H); ^{77}Se NMR (76 MHz, $CDCl_3$, δ, ppm, Me_2Se): 821.3. Anal. Calc. for **1** (OO) ($C_{12}H_{12}O_2Se_2$): C, 41.64; H, 3.49%. Found: C, 41.55; H, 3.45%. Anal. Calc. for **1** (OO)·2.5H_2O ($C_{24}H_{24}O_4Se_4$·5H_2O): C, 36.84; H, 4.38%. Found: C, 36.87; H, 4.41%.

1,8-Bis(ethylselanyl)naphthalene (2 (LL)). Following the similar method to that used for **1** (LL), **2** (LL) gave 80% yield as colorless powder, mp 52.3–52.8 °C; ^1H NMR (400 MHz, $CDCl_3$, δ, ppm, TMS): 1.35 (t, J 7.4 Hz, 6H), 2.89 (q, J 7.5 Hz, 4H), 7.32 (t, J 7.6 Hz, 2H), 7.70 (dd, J 1.2 and 8.1 Hz, 2H), 7.76 (dd, J 1.1 and 7.2 Hz, 2H); ^{77}Se NMR (76 MHz, $CDCl_3$, δ, ppm, Me_2Se): 341.7. Anal. Calc. for **2** (LL) ($C_{14}H_{16}Se_2$): C, 49.14; H, 4.71%. Found: C, 49.23; H, 4.72%.

8-Phenylselanyl-1-(methylseleninyl)naphthalene (3a (LO)). Following the similar method to that used for **1** (LO), **3a** (LO) gave 80% yield as colorless needles, mp 129.8–130.2 °C; ^1H NMR (400 MHz, $CDCl_3$, δ, ppm, TMS): 2.72 (s, 3H), 6.98–7.02 (m, 2H), 7.11–7.16 (m, 3H), 7.56 (t, J 7.6 Hz, 1H), 7.76 (t, J 7.7 Hz, 1H), 8.05 (dd, J 1.2 and 8.0 Hz, 1H), 8.10 (dd, J 1.3 and 8.1 Hz, 1H), 8.15 (dd, J 1.3 and 7.2 Hz, 1H), 8.82 (dd, J 1.3 and 7.3 Hz, 1H); ^{13}C NMR (75 MHz, $CDCl_3$, δ, ppm, TMS) 40.56, 123.19, 126.51, 126.57, 126.75, 126.88, 128.42 (^2J(Se,C) 5.9 Hz), 129.63, 131.95, 132.42, 133.03, 133.50, 136.29, 140.89, 141.37; ^{77}Se NMR (76 MHz, $CDCl_3$, δ, ppm, Me_2Se): 398.2, 831.4. Anal. Calc. for **3a** (LO) ($C_{17}H_{14}OSe_2$): C, 52.06; H, 3.60%. Found: C, 52.11; H, 3.66%.

8-Phenylseleninyl-1-(methylseleninyl)naphthalene (3a (OO)). Following the similar method to that used for **1** (OO), **3a** (OO) gave 63% yield as colorless needles, mp 148.0–148.8 °C; ^{1}H NMR (400 MHz, $CDCl_3$, δ, ppm, TMS): 2.74 (s, 3H), 7.33–7.50 (m, 3H), 7.51–7.58 (m, 2H), 7.78 (t, *J* 7.7 Hz, 1H), 7.81 (t, *J* 7.7 Hz, 1H), 8.13 (dd, *J* 1.1 and 8.1 Hz, 1H), 8.14 (dd, *J* 1.1 and 8.1 Hz, 1H), 8.63 (dd, *J* 1.4 and 7.4 Hz, 1H), 8.72 (dd, *J* 1.3 and 7.3 Hz, 1H); ^{13}C NMR (75 MHz, $CDCl_3$, δ, ppm, TMS): 38.25, 126.72, 126.80, 126.85, 127.01, 127.64, 127.92, 130.02, 131.70, 133.33, 133.71, 135.55, 138.88, 139.22, 141.66; ^{77}Se NMR (76 MHz, $CDCl_3$, δ, ppm, Me_2Se): 820.0, 832.5. Anal. Calc. for **3a** (OO) ($C_{17}H_{14}O_2Se_2$): C, 50.02; H, 3.46%. Found: C, 50.07; H, 3.57%.

8-*p*-Anisylselanyl-1-(methylseleninyl)naphthalene (3b (LO)). Following the similar method to that used for **1** (LO), **3b** (LO) gave 88% yield as colorless needles, mp 129.6–130.4 °C; ^{1}H NMR (400 MHz, $CDCl_3$, δ, ppm, TMS): 2.70 (s, 3H), 3.82 (s, 3H), 6.70 (d, *J* 8.8 Hz, 2H), 7.01 (d, *J* 8.8 Hz, 2H), 7.51 (t, *J* 7.2 Hz, 1H), 7.74 (t, *J* 7.2 Hz, 1H), 7.88 (dd, *J* 1.1 and 6.8 Hz, 1H), 8.01 (dd, *J* 1.1 and 6.8 Hz, 1H), 8.03 (dd, *J* 1.1 and 6.8 Hz, 1H), 8.10 (dd, *J* 1.1 and 6.8 Hz, 1H); ^{77}Se NMR (76 MHz, $CDCl_3$, δ, ppm, Me_2Se): 385.9, 833.9. Anal. Calc. for **3b** (LO) ($C_{18}H_{16}O_2Se_2$): C, 51.20; H, 3.82%. Found: C, 50.98; H, 3.83%.

8-*p*-Anisylseleninyl-1-(methylseleninyl)naphthalene (3b (OO)). Following the similar method to that used for **1** (OO), **3b** (OO) gave 43% yield as colorless powder, mp 144.5–145.0 °C; ^{1}H NMR (400 MHz, $CDCl_3$, δ, ppm, TMS): 2.75 (s, 3H), 3.76 (s, 3H), 6.87 (d, *J* 8.9 Hz, 2H), 7.45 (d, *J* 8.9 Hz, 2H), 7.83 (t, *J* 7.7 Hz, 2H), 8.15 (dd, *J* 1.0, 8.2 Hz, 1H), 8.17 (dd, *J* 1.0, 8.2 Hz, 1H), 8.69 (dd, *J* 1.3, 9.1 Hz, 1H), 8.71 (dd, *J* 1.2, 9.1 Hz, 1H); ^{77}Se NMR (76 MHz, $CDCl_3$, δ, ppm, Me_2Se): 821.6, 846.4. Anal. Calc. for **3b** (OO) ($C_{18}H_{16}O_3Se_2$): C, 49.33; H, 3.68%. Found: C, 49.30; H, 3.73%.

8-*p*-Nitrophenylselanyl-1-(methylseleninyl)naphthalene (3d (LO)). Following the similar method to that used for **1** (LO), **3d** (LO) gave 61% yield as colorless powder, mp 141.5–142.0 °C; ^{1}H NMR (400 MHz, $CDCl_3$, δ, ppm, TMS): 2.67 (s, 3H), 7.07 (dt, *J* 2.1 and 9.0 Hz, 2H), 7.64 (t, *J* 7.5 Hz, 1H), 7.83 (t, *J* 7.5 Hz, 1H), 7.99 (dt, *J* 2.4 and 9.0 Hz, 2H), 8.11 (dd, *J* 1.2 and 6.9 Hz, 2H), 8.18 (dd, *J* 1.2 and 4.2 Hz, 1H), 8.21 (dd, *J* 1.5 and 4.8 Hz, 1H), 8.84 (dd, *J* 1.2 and 6.0 Hz, 1H); ^{77}Se NMR (76 MHz, $CDCl_3$, δ, ppm, Me_2Se): 426.4, 835.6. Anal. Calc. for **3d** (LO) ($C_{17}H_{13}NO_3Se_2$): C, 46.70; H, 3.00; N, 3.20%. Found: C, 46.75; H, 3.03; N, 3.22%.

8-*p*-Nitrophenylseleninyl-1-(methylseleninyl)naphthalene (3d (OO)). Following the similar method to that used for **1** (OO), **3d** (OO) gave 82% yield as colorless powder, mp 151.2–152.0 °C; ^{1}H NMR (400 MHz, $CDCl_3$, δ, ppm, TMS): 2.83 (s, 3H), 7.72–7.92 (m, 4H), 8.12–8.27 (m, 4H), 8.57 (dd, *J* 1.1 and 6.2 Hz, 1H), 8.74 (dd, *J* 1.3 and 6.1 Hz, 1H); ^{77}Se NMR (76 MHz, $CDCl_3$, δ, ppm, Me_2Se): 821.4, 849.0. Anal. Calc. for **3d** (OO) ($C_{17}H_{13}NO_4Se_2$): C, 45.05; H, 2.89; N, 3.09%. Found: C, 45.12; H, 2.83; N, 3.12%.

1,8-Bis(phenylselanyl)naphthalene (4a (LL)). Under an argon atmosphere, 1,8-diiodonaphthalene (4.33 g, 11.40 mmol) was dissolved in 100 mL of dry THF and the solution was added to *n*BuLi (15.0 mL, 23.94 mmol, 1.6 N) at −78 °C. After 20 min, a THF solution of phenylselenobromide (22.80 mmol) was added to the above solution at −78 °C. Then the reaction mixture was stirring for 2 h and warmed up room temperature. Then, 20 mL of 5% acetone hydrochloric acid and 100 mL of benzene were added. The organic layer was separated, washed with brine, 10% aqueous solution of sodium hydroxide, saturated aqueous solution of sodium bicarbonate and brine. Then the solution was dried over sodium sulfate, evaporated and dried *in vacuo*. The crude product was purified by column chromatography (flash column, SiO_2, hexane). **4a** (LL) gave 89% yield as yellow prisms, mp 64.0–64.8 °C; ^{1}H NMR (300 MHz, $CDCl_3$, δ, ppm, TMS): 7.22–7.28 (m, 8H), 7.39–7.45 (m, 4H), 7.64 (dd, *J* 1.1 and 7.3 Hz, 2H), 7.74 (dd, *J* 1.1 and 8.3 Hz, 2H); ^{13}C NMR (75 MHz, $CDCl_3$, δ, ppm, TMS): 126.0, 127.4, 129.2, 129.4, 131.4, 133.4, 135.18, 135.19, 135.5, 135.9; ^{77}Se NMR (76 MHz, $CDCl_3$, δ, ppm, Me_2Se): 435.4. Anal. Calc. for **4a** (LL) ($C_{22}H_{16}Se_2$): C, 60.29; H, 3.68%. Found: C, 60.21; H, 3.75%.

8-Phenylselanyl-1-(phenylseleninyl)naphthalene (4a (LO)). Following the similar method to that used for **1** (LO), **4a** (LO) gave 65% yield as colorless prisms, mp 155.5–156.3 °C; ^{1}H NMR (400 MHz, $CDCl_3$, δ, ppm, TMS): 6.90–6.95 (m, 4H), 7.10–7.13 (m, 6H), 7.22–7.26 (m, 6H), 7.48–7.53 (m, 4H), 7.52 (t, *J* 8.2 Hz, 1H), 7.83 (d, *J* 7.7 Hz, 1H), 8.07 (dd, *J* 1.3 and 7.2 Hz, 1H), 8.08 (dd, *J* 1.3 and 8.2 Hz, 1H), 9.02 (dd, *J* 1.3 and 7.3 Hz, 1H); ^{13}C NMR (75 MHz, $CDCl_3$, δ, ppm, TMS): 123.90, 126.45, 126.51, 126.79, 127.86, 127.91, 128.70, 129.17, 129.49, 130.11, 131.73, 132.76, 133.27, 133.78, 136.31, 140.17, 140.71, 146.21; ^{77}Se NMR (76 MHz, $CDCl_3$, δ, ppm, Me_2Se): 400.1, 863.7. Anal. Calc. for **4a** (LO) ($C_{22}H_{16}OSe_2$): C, 58.17; H, 3.55%. Found: C, 58.11; H, 3.65%.

1,8-Bis(phenylseleninyl)naphthalene (4a (OO)). Following the similar method to that used for **1** (OO), **4a** (OO) gave 78% yield as colorless prisms, mp. 187.5–188.3 °C; ^{1}H NMR (400 MHz, $CDCl_3$, δ, ppm, TMS): 7.21–7.30 (m, 8H), 7.37 (tt, *J* 1.5 and 6.8 Hz, 2H), 7.76 (t, *J* 7.7 Hz, 2H), 8.15 (dd, *J* 0.9 and 7.5 Hz, 2H), 8.47 (dd, *J* 1.1 and 6.2 Hz, 2H); ^{77}Se NMR (76 MHz, $CDCl_3$, δ, ppm, Me_2Se): 877.1. Anal. Calc. for **4a** (OO) ($C_{22}H_{16}O_2Se_2$): C, 56.19; H, 3.43%. Found: C, 56.22; H, 3.53%.

1,8-Bis[(*p*-*tert*-butylphenyl)selanyl]naphthalene (4c (LL)). Following the similar method to that used for **4a** (LL), **4c** (LL) gave 87% yield as yellow prisms, mp 97.8–98.3 °C; ^{1}H NMR (400 MHz, $CDCl_3$, δ, ppm, TMS): 1.30 (s 18H), 7.24 (t, *J* 7.7 Hz, 2H), 7.27 (d, *J* 8.6 Hz, 4H), 7.38 (d, *J* 8.6 Hz, 4H), 7.65 (dd, *J* 1.3 and 6.1 Hz, 2H), 7.73 (dd, *J* 1.3 and 7.0 Hz, 2H); ^{77}Se NMR (76 MHz, $CDCl_3$, δ, ppm, Me_2Se): 424.6. Anal. Calc. for **4c** (LL) ($C_{30}H_{32}Se_2$): C, 65.45; H, 5.86%. Found: C, 65.41; H, 5.88%.

8-[(*p*-*tert*-Butylphenyl)selanyl]-1-[(*p*-*tert*-butylphenyl)seleninyl]-naphthalene (4c (LO)). Following the similar method to that used for **1** (LO), **4c** (LO) gave 86% yield as colorless powder, mp 179.5–180.2 °C; ^{1}H NMR (400 MHz, $CDCl_3$, δ, ppm, TMS): 1.22 (s, 9H), 1.27 (s 9H), 6.91 (d, *J* 8.3 Hz, 2H),

7.15 (d, *J* 8.1 Hz, 2H), 7.28 (d, *J* 8.8 Hz, 2H), 7.43 (d, *J* 8.6 Hz, 2H), 7.51 (t, *J* 7.9 Hz, 1H), 7.82 (t, *J* 7.7 Hz, 1H), 8.07 (d, *J* 8.3 Hz, 3H), 9.01 (dd, *J* 1.3 and 7.5 Hz, 1H); ^{77}Se NMR (76 MHz, $CDCl_3$, δ, ppm, Me_2Se): 393.2, 861.2. Anal. Calc. for **4c** (LO) ($C_{30}H_{32}OSe_2$): C, 63.61; H, 5.69%. Found: C, 63.55; H, 5.58%.

1,8-Bis[(*p*-*tert*-butylphenyl)seleninyl]naphthalene (4c (OO)). Following the similar method to that used for **1** (OO), **4c** (OO) gave 87% yield as colorless powder, mp 172.5–173.2 °C; ^{1}H NMR (400 MHz, $CDCl_3$, δ, ppm, TMS): 1.63 (s, 18H), 7.39 (d, *J* 8.6 Hz, 4H), 7.47 (d, *J* 8.3 Hz, 4H), 7.83 (d, *J* 7.6 Hz, 2H), 8.16 (dd, *J* 0.8 and 7.3 Hz, 2H), 8.73 (dd, *J* 1.0 and 6.2 Hz, 2H); ^{77}Se NMR (76 MHz, $CDCl_3$, δ, ppm, Me_2Se): 843.7. Anal. Calc. for **4c** (OO) ($C_{30}H_{32}O_2Se_2$): C, 61.86; H, 5.54%. Found: C, 61.93; H, 5.58%.

1-(Methylselanyl)naphthalene (5 (L)). Following the similar method to that used for **1** (LL), **5** (L) gave 99% yield as pale yellow oil; ^{1}H NMR (400 MHz, $CDCl_3$, δ, ppm, TMS): 2.37 (s, $^2J_{Se,H}$ 11.7 Hz, 3H), 7.35 (dd, *J* 7.3 and 8.1 Hz, 1H), 7.47 (ddd, *J* 1.6, 6.9 and 8.2 Hz, 1H), 7.53 (ddd, *J* 1.6, 6.9 and 8.3 Hz, 1H), 7.66 (dd, *J* 1.1 and 7.3 Hz, 1H), 7.71 (d, *J* 8.2 Hz, 1H), 7.80 (dd, *J* 1.7 and 7.9 Hz, 1H), 8.24 (ddd, *J* 0.7, 1.6 and 8.1 Hz, 1H); ^{13}C NMR (75 MHz, $CDCl_3$, δ, ppm, TMS): 36.54, 122.08 (*J* 14.9 Hz), 124.03 (*J* 6.2 Hz), 126.11, 126.79, 127.56, 129.35, 130.27, 131.40, 133.88, 138.68; ^{77}Se NMR (76 MHz, $CDCl_3$, δ, ppm, Me_2Se): 158.6. Anal. Calc. for **5** (L) ($C_{11}H_{10}Se$): C, 59.74; H, 4.56%. Found: C, 59.90; H, 4.49%.

1-(Methylseleninyl)naphthalene (5 (O)). Following the similar method to that used for **1** (LO), **5** (O) gave 67% yield as colorless needles, mp 97.2–97.8 °C; ^{1}H NMR (400 MHz, $CDCl_3$, δ, ppm, TMS): 2.71 (s, $^2J_{Se,H}$ 12.3 Hz, 3H), 7.56–7.65 (m, 2H), 7.70 (dd, *J* 7.4 and 8.2 Hz, 1H), 7.81–7.87 (m, 1H), 7.95–8.02 (m, 2H), 8.29 (dd, *J* 1.1 and 7.3 Hz, 1H); ^{13}C NMR (75 MHz, $CDCl_3$, δ, ppm, TMS): 7.52, 125.83, 126.14, 126.39, 126.63, 127.16, 128.58, 128.67, 131.10, 133.29, 133.77; ^{77}Se NMR (76 MHz, $CDCl_3$, δ, ppm, Me_2Se): 809.3. Anal. Calc. for **5** (O) ($C_{11}H_{10}OSe$): C, 55.71; H, 4.25%. Found: C, 55.88; H, 4.18%.

X-Ray crystal structure determination. The colorless crystals of **1** (LO) and **1** (OO) were grown by slow evaporation of methylene dichloride-hexane solutions at room temperature. A crystal of **1** (LO) was measured on a Rigaku AFC5R diffractometer with graphite monochromated Mo-Kα radiation source (λ = 0.71069 Å) and a rotating anode generator at 298(2) K. That of **1** (OO) was measured on a Rigaku/MSC Mercury CCD diffractometer equipped with a graphite-monochromated Mo-Kα radiation source (λ = 0.71070 Å) at 103(2) K. The structures of **1** (LO) and **1** (OO) were solved by direct method (SHELXS-97)[41] and refined by full-matrix least-square method on F^2 for all reflections (SHELXL-97).[42] All the non-hydrogen atoms were refined anisotropically.

QC calculations

QC calculations are performed on **1** (LO) and **1** (OO), as the models of ***n*** (LO) and ***n*** (OO) (***n*** = **1**, **3** and **4**), respectively, employing the 6-311 + G(d) basis sets of the Gaussian 98 program.[27] Calculations are performed at the density functional theory (DFT) level of the Becke three parameter hybrid functionals combined with the Lee-Yang-Parr correlation functional (B3LYP).[28,29] QC calculations are also performed on 8-G-1-[MeSe(X)]$C_{10}H_6$ [G = MeSe (**1**), H (**5**), F (**6**), Cl (**7**) and Br (**8**) with X = lone pair (L), O (O), OH^+ (OH^+) and O_2H_2 (OH·OH)], employing the B3LYP/6-311 + G(d) method. The NBO[19,20] analysis were performed with the B3LYP/6-311 + G(d) method. The AIM[21,22] analysis are performed on **1** (LO) and **1** (OO) with the Gaussian 03 program employing the 6-311 + G(3df) basis sets for Se with the 6-311 + G(3d,2p) basis sets for C and H at the B3LYP level. They are analyzed employing the AIM 2000 program.[21,22] NBO analysis are also performed on **1** (LO) and **1** (OO) with the same method for the AIM analysis. Optimized structures and the molecular orbitals are drawn using MolStudio *R3.2* (*Rev 1.0*).[43]

Acknowledgements

This work was partially supported by a Grant-in-Aid for Scientific Research (Nos. 16550038, 19550041 and 20550042) from the Ministry of Education, Culture, Sports, Science and Technology, Japan.

References

1 (*a*) *The Chemistry of Organic Selenium and Tellurium Compounds*, eds. S. Patai and Z. Rappoport, John-Wiley and Sons, New York, 1986, vol. 1; (*b*) *The Chemistry of Organic Selenium and Tellurium Compounds*, ed. S. Patai, John-Wiley and Sons, New York, 1986, vol. 2; (*c*) *Organoselenium Chemistry, A Practical Approach*, ed. T. G. Back, Oxford University Press, Oxford, 1999. See also refs cited therein.
2 T. Shimizu and N. Kamigata, *Synthesis and Stereochemistry of Optically Active Chalcogen Compounds*, in *Handbook of Chalcogen Chemistry New Perspectives in Sulfur Selenium and Tellurium*, ed. F. A. Devillanova, Royal Society of Chemistry, Cambridge, 2006, ch. 10.1.
3 (*a*) P. Nagy, A. Csampai, D. Szabo, J. Varga, V. Harmat, F. Ruff and A. Kucsman, *J. Chem. Soc., Perkin Trans. 2*, 2001, 339–349; (*b*) C. Reichardt, H.-P. Erfurt, K. Harms and G. Schafer, *Eur. J. Org. Chem.*, 2002, 439–452.
4 (*a*) T. Shimizu, M. Enomoto, H. Taka and N. Kamigata, *J. Org. Chem.*, 1999, **64**, 8242–8247; (*b*) H. Taka, A. Matsumoto, T. Shimizu and N. Kamigata, *Chem. Lett.*, 2000, 726–727; (*c*) H. Taka, Y. Yamazaki, T. Shimizu and N. Kamigata, *J. Org. Chem.*, 2000, **65**, 2127–2133; (*d*) H. Taka, A. Matsumoto, T. Shimizu and N. Kamigata, *Heteroat. Chem.*, 2001, **12**, 227–237; (*e*) T. Soma, T. Shimizu, K. Hirabayashi and N. Kamigata, *Heteroat. Chem.*, 2007, **18**, 301–311; (*f*) T. Soma, N. Kamigata, K. Hirabayashi and T. Shimizu, *Bull. Chem. Soc. Jpn.*, 2007, **80**, 2389–2394. For the N···Si interactions at naphthalene 1,8-positions, see: P. M. Dominiak, G. P. Schiemenz and K. Woz'niak, *Pol. J. Chem.*, 2007, **81**, 663–681.
5 *Organic Sulfur Chemistry: Theoretical and Experimental Advances*, eds. F. Bernardi, I. G. Csizmadia and A. Mangini, Elsevier, Amsterdam, 1985.
6 (*a*) S. Nakamura, H. Yasuda and T. Toru, *Tetrahedron: Asymmetry*, 2002, **13**, 1509–1518; (*b*) S. Nakamura, H. Yasuda, Y. Watanabe and T. Toru, *J. Org. Chem.*, 2000, **65**, 8640–8650; (*c*) S. Nakamura, H. Yasuda, Y. Watanabe and T. Toru, *Tetrahedron Lett.*, 2000, **41**, 4157–4160.
7 (*a*) J. Drabowicz, *Hypervalent Sulfuranes as Transient and Isolable Structures: Occurrence, Synthesis, and Reactivity in Chemistry of Hypervalent Compounds*, ed. K.-y. Akiba, Wiley-VCH, New York, 1999, ch. 7; (*b*) J. Drabowicz, *Heteroat. Chem.*, 2002, **5**, 437–442.
8 (*a*) W. Nakanishi, *Chem. Lett.*, 1993, 2121–2122; (*b*) W. Nakanishi, S. Hayashi and S. Toyota, *Chem. Commun.*, 1996, 371–372; (*c*) W. Nakanishi, S. Hayashi and H. Yamaguchi, *Chem. Lett.*,

1996, 947–948; (*d*) W. Nakanishi, S. Hayashi, A. Sakaue, G. Ono and Y. Kawada, *J. Am. Chem. Soc.*, 1998, **120**, 3635–3640; (*e*) W. Nakanishi, S. Hayashi and S. Toyota, *J. Org. Chem.*, 1998, **63**, 8790–8800; (*f*) S. Hayashi and W. Nakanishi, *J. Org. Chem.*, 1999, **64**, 6688–6696; (*g*) W. Nakanishi, S. Hayashi and T. Uehara, *J.Phys. Chem. A*, 1999, **103**, 9906–9912; (*h*) W. Nakanishi and S. Hayashi, *J. Org. Chem.*, 2002, **67**, 38–48.

9 (*a*) G. Gafner and F. H. Herbstein, *Acta. Crystallogr.*, 1962, **15**, 1081–1092; (*b*) M. A. Davydova and Yu. T. Struchkov, *Zh. Strukt. Khim.*, 1962, **3**, 184; (*c*) M. A. Davydova and Yu. T. Struchkov, *Zh. Strukt. Khim.*, 1968, **9**, 1968; (*d*) H. Bock, M. Sievert and Z. Havlas, *Chem. Eur. J.*, 1998, **4**, 677–685; (*e*) R. D. Jackson, S. James, A. G. Orpen and P. G. Pringle, *J. Organomet. Chem.*, 1993, **458**, C3–C4; G. Mugesh and H. B. Singh, *Acc. Chem. Rev.*, 2002, **35**, 226–236.

10 (*a*) R. S. Glass, S. W. Andruski, J. L. Broeker, H. Firouzabadi, L. K. Steffen and G. S. Wilson, *J. Am. Chem. Soc.*, 1989, **111**, 4036–4045; (*b*) R. S. Glass, L. Adamowicz and J. L. Broeker, *J. Am. Chem. Soc.*, 1991, **113**, 1065–1072; (*c*) F. B. Mallory, C. W. Mallory, K. B. Butler, M. B. Lewis, A. Q. Xia, E. D. Luzik, Jr, L. E. Fredenburgh, M. M. Ramanjulu, Q. N. Van, M. M. Francl, D. A. Freed, C. C. Wray, C. Hann, M. Nerz-Stormes, P. J. Carroll and L. E. Chirlian, *J. Am. Chem. Soc.*, 2000, **122**, 4108–4116.

11 (*a*) A. Singh and B. Ganguly, *J. Phys. Chem. A*, 2007, **111**, 6468–6471; (*b*) N. Chanda and P. R. Sharp, *Organometallics*, 2007, **26**, 3368–3373; (*c*) R. Panisch, M. Bolte and T. Muller, *Organometallics*, 2007, **26**, 3524–3529; (*d*) A. F. Pozharskii, A. V. Degtyarev, O. V. Ryabtsova, V. A. Ozeryanskii, M. E. Kletskii, Z. A. Starikova, L. Sobczyk and A. Filarowski, *J. Org. Chem.*, 2007, **72**, 3006–3019.

12 (*a*) G. C. Pimentel, *J. Chem. Phys.*, 1951, **19**, 446–448; J. I. Musher, *Angew. Chem., Int. Ed. Engl.*, 1969, **8**, 54–68; R. J. Hatch and R. E. Rundle, *J. Am. Chem. Soc.*, 1951, **73**, 4321–4324; (*b*) R. E. Rundle, *J. Am. Chem. Soc.*, 1963, **85**, 112–113.

13 (*a*) R. A. Hayes and J. C. Martin, *Sulfurane Chemistry*, in *Organic Sulfur Chemistry: Theoretical and Experimental Advances*, eds. F. Bernardi, I. G. Csizmadia and A. Mangini, Elsevier Scientific, Amsterdam, 1985, ch. 8; (*b*) J. Bergman, L. Engman and J. Siden, *Tetra- and Higher-Valent (Hypervalent) Derivatives of Selenium and Tellurium*, in *The Chemistry of Organic Selenium and Tellurium Compounds*, eds. S. Patai and Z. Rappoport, John Wiley & Sons, New York, 1986, vol. 1, ch. 14; (*c*) *Chemistry of Hypervalent Compounds*, ed. K.-y. Akiba, Wiley-VCH, New York, 1999; (*d*) W. Nakanishi, *Hypervalent Chalcogen Compounds*, in *Handbook of Chalcogen Chemistry: New Perspectives in Sulfur, Selenium and Tellurium*, ed. F. A. Devillanova, Royal Society of Chemistry, London, 2006, ch. 10.3.

14 For the 3c–4e treatment of the CT complexes, see: W. Nakanishi, S. Hayashi and H. Kihara, *J. Org. Chem.*, 1999, **64**, 2630–2637.

15 For the weak interactions, see, (*a*) *Molecular Interactions. From van der Waals to Strongly Bound Complexes*, ed. S. Scheiner, Wiley, New York, 1997; (*b*) K. D. Asmus, *Acc. Chem. Res.*, 1979, **12**, 436–442; (*c*) W. K. Musker, *Acc. Chem. Res.*, 1980, **13**, 200–206.

16 S. Hayashi, H. Wada, T. Ueno and W. Nakanishi, *J. Org. Chem.*, 2006, **71**, 5574–5585.

17 W. Nakanishi, S. Hayashi and T. Uehara, *Eur. J. Org. Chem.*, 2001, 3933–3943.

18 The structure is **A** if the Se–C_{Ar} bond is placed almost perpendicular to the naphthyl plane, it is **B** when the bond is located on the plane and **C** is the intermediate between **A** and **B**.

19 A. E. Reed, R. B. Weinstock and F. Weinhold, *J. Chem. Phys.*, 1985, **83**, 735–746; J. E. Carpenter and F. Weinhold, *J. Mol. Struct. (THEOCHEM)*, 1988, **169**, 41–62.

20 E. D. Glendening, A. E. Reed, J. E. Carpenter and F. Weinhold, NBO Ver. 3.1.

21 *Atoms in Molecules. A Quantum Theory*, ed. R. F. W. Bader, Oxford University Press, Oxford, 1990; *The Quantum Theory of Atoms in Molecules: From Solid State to DNA and Drug Design*, eds. C. F. Matta and R. J. Boyd, Wiley-VCH, Weinheim, 2007, ch. 1.

22 (*a*) R. F. W. Bader, T. S. Slee, D. Cremer and E. Kraka, *J. Am. Chem. Soc.*, 1983, **105**, 5061–5068; (*b*) R. F. W. Bader, *Chem. Rev.*, 1991, **91**, 893–926; (*c*) R. F. W. Bader, *J. Phys. Chem. A*, 1998, **102**, 7314–7323; (*d*) F. Biegler-König, R. F. W. Bader and T. H. Tang, *J. Comput. Chem.*, 1982, **3**, 317–328; (*e*) R. F. W. Bader, *Acc. Chem. Res.*, 1985, **18**, 9–15; (*f*) T. H. Tang, R. F. W. Bader and P. MacDougall, *Inorg. Chem.*, 1985, **24**, 2047–2053; (*g*) F. Biegler-König, J. Schönbohm and D. Bayles, *J. Comput. Chem.*, 2001, **22**, 545–559; (*h*) F. Biegler-König and J. Schönbohm, *J. Comput. Chem.*, 2002, **23**, 1489–1494. See also: W. Nakanishi, T. Nakamoto, S. Hayashi, T. Sasamori and N. Tokitoh, *Chem. Eur. J.*, 2007, **13**, 255–268.

23 J. Meinwald, D. Dauplaise and J. Clardy, *J. Am. Chem. Soc.*, 1977, **99**, 7743–7744.

24 The structures of **3b** (LO) and **3a** (OO) are also determined by the X-ray crystallographic analysis. The results are essentially the same as those of **1** (LO) and **1** (OO), respectively, which will be reported elsewhere.

25 Water molecules in **1** (OO) are omitted for clarity.

26 S. Hayashi and W. Nakanishi, *Bull. Chem. Soc. Jpn.*, 2008, **12**, in press (CCDC 640537 for **1** (LL)).

27 A. Bondi, *J. Phys. Chem.*, 1964, **68**, 441–451.

28 M. J. Frisch, G. W. Trucks, H. B. Schlegel, G. E. Scuseria, M. A. Robb, J. R. Cheeseman, V. G. Zakrzewski, J. A. Montgomery, Jr., R. E. Stratmann, J. C. Burant, S. Dapprich, J. M. Millam, A. D. Daniels, K. N. Kudin, M. C. Strain, O. Farkas, J. Tomasi, V. Barone, M. Cossi, R. Cammi, B. Mennucci, C. Pomelli, C. Adamo, S. Clifford, J. Ochterski, G. A. Petersson, P. Y. Ayala, Q. Cui, K. Morokuma, P. Salvador, J. J. Dannenberg, D. K. Malick, A. D. Rabuck, K. Raghavachari, J. B. Foresman, J. Cioslowski, J. V. Ortiz, A. G. Baboul, B. B. Stefanov, G. Liu, A. Liashenko, P. Piskorz, I. Komaromi, R. Gomperts, R. L. Martin, D. J. Fox, T. Keith, M. A. Al-Laham, C. Y. Peng, A. Nanayakkara, M. Challacombe, P. M. W. Gill, B. G. Johnson, W. Chen, M. W. Wong, J. L. Andres, C. Gonzalez, M. Head-Gordon, E. S. Replogle and J. A. Pople, *GAUSSIAN 98 (Revision A.11)*, Gaussian, Inc., Pittsburgh, PA, 2001.

29 C. Lee, W. Yang and R. G. Parr, *Phys. Rev. B*, 1988, **37**, 785–789; B. Miehlich, A. Savin, H. Stoll and H. Preuss, *Chem. Phys. Lett.*, 1989, **157**, 200–2006.

30 A. D. Becke, *Phys. Rev. A*, 1988, **38**, 3098–3100; A. D. Becke, *J. Chem. Phys.*, 1993, **98**, 5648–5652.

31 S. Hayashi and W. Nakanishi, *J. Mol. Struct. (THEOCHEM)*, 2007, **811**, 293–301.

32 M. J. Frisch, G. W. Trucks, H. B. Schlegel, G. E. Scuseria, M. A. Robb, J. R. Cheeseman, J. A. Montgomery, Jr, T. Vreven, K. N. Kudin, J. C. Burant, J. M. Millam, S. S. Iyengar, J. Tomasi, V. Barone, B. Mennucci, M. Cossi, G. Scalmani, N. Rega, G. A. Petersson, H. Nakatsuji, M. Hada, M. Ehara, K. Toyota, R. Fukuda, J. Hasegawa, M. Ishida, T. Nakajima, Y. Honda, O. Kitao, H. Nakai, M. Klene, X. Li, J. E. Knox, H. P. Hratchian, J. B. Cross, V. Bakken, C. Adamo, J. Jaramillo, R. Gomperts, R. E. Stratmann, O. Yazyev, A. J. Austin, R. Cammi, C. Pomelli, J. W. Ochterski, P. Y. Ayala, K. Morokuma, G. A. Voth, P. Salvador, J. J. Dannenberg, V. G. Zakrzewski, S. Dapprich, A. D. Daniels, M. C. Strain, O. Farkas, D. K. Malick, A. D. Rabuck, K. Raghavachari, J. B. Foresman, J. V. Ortiz, Q. Cui, A. G. Baboul, S. Clifford, J. Cioslowski, B. B. Stefanov, G. Liu, A. Liashenko, P. Piskorz, I. Komaromi, R. L. Martin, D. J. Fox, T. Keith, M. A. Al-Laham, C. Y. Peng, A. Nanayakkara, M. Challacombe, P. M. W. Gill, B. Johnson, W. Chen, M. W. Wong, C. Gonzalez and J. A. Pople, *GAUSSIAN 03 (Revision B.05)*, Gaussian, Inc., Pittsburgh, PA, 2003.

33 The AIM2000 program (Version 2.0) is employed to analyze and visualize atoms in molecules: F. J. Biegler-König, *Comput. Chem.*, 2000, **21**, 1040–1048; see also ref. 22*g*.

34 Data for **A** and **B**, together with LL, are given in the ESI†.

35 The type **C** of **1** (OH·OH) is discussed which is predicted to be most stable among the three[44].

36 Eqn (R1) shows the energies of $\boldsymbol{n}$(L) + H_2O_2 ($E(\boldsymbol{n}(L) + H_2O_2)$) relative to $E(\boldsymbol{n}(O) + H_2O)$ [$\Delta E(\boldsymbol{n}(LO)) = E(\boldsymbol{n}(L) + H_2O_2) - E(\boldsymbol{n}(O) + H_2O)$], although $E(\boldsymbol{n}(L))$ are not given in Table 3.[45]

$$\Delta E(\boldsymbol{n}(LO)) = E(\boldsymbol{n}(L) + H_2O_2) - E(\boldsymbol{n}(O) + H_2O)$$
$$G = H\ (121.8\ kJ\ mol^{-1}) < F\ (131.3) < \textit{cis}\text{-MeSe}\ (133.9) < Cl\ (136.8) \leq Br\ (137.6) < \textit{trans}\text{-MeSe}\ (141.0) \qquad (R1)$$

37 NOB analysis were also performed on the **AC** conformer of 8-G-1-[$MeSe(O_2H_2)$]$C_{10}H_6$. However, the corresponding CT interactions were not detected.

38 The nonbonded Se···Se distance in **1**(LO) is predicted to be shorter than that of **1**(OO) by *ca.* 0.03 Å, while the observed values are almost equal (see Table 5). The crystal packing effect might contribute to the results.
39 The value is very close to that evaluated with the B3LYP/6-311+G(d) method.
40 W. Nakanishi, S. Hayashi and K. Narahara, unpublished results.
41 G. M. Sheldrick, SHELXS-97, Program for Crystal Structure Solution, Universität Göttingen, Germany, 1997.
42 G. M. Sheldrick, SHELXL-97, Program for Crystal Structure Refinement, University of Göttingen, Germany, 1997.
43 MolStudio R3.2 (Rev 1.0), NEC Corporation, 1997–2003.
44 Three structures (type **A**, type **B** and type **C**) were optimized for each of ***n***(OH·OH). The type **C** is the global minimum, which is slightly stable than type **B** and much stable than type **A**, although the steric repulsion between OH and G seems largest.
45 Eqn (R1)[36] shows that selenoxides are stabilized in this order through the non-bonded n(G)···σ*(Se–O) 3c–4e interactions, together with the O dependence.[16] While G = *trans*-MeSe is demonstrated to be most effective to stabilize in the selenoxide relative to the corresponding bis-selenide, the effect of G = *cis*-MeSe places between F and Cl, where the **CC** form is postulated for the bis-selenide.

